Journal of Structural Biology 194 (2016) 191–198

Contents lists available at ScienceDirect

Journal of Structural Biology

journal homepage: www.elsevier.com/locate/yjsbi

Cholesteryl ester transfer between lipoproteins does not require a ternary tunnel complex with CETP

Matthias E. Lauer [a,1], Alexandra Graff-Meyer [b,1], Arne C. Rufer [a], Cyrille Maugeais [a], Elisabeth von der Mark [a], Hugues Matile [a], Brigitte D'Arcy [a], Christine Magg [a,c], Philippe Ringler [b], Shirley A. Müller [b], Sebastian Scherer [b], Gregor Dernick [a], Ralf Thoma [a], Michael Hennig [a,d], Eric J. Niesor [a,*], Henning Stahlberg [b,*]

[a] Pharma Research and Early Development, pRED, Roche Innovation Center Basel, F. Hoffmann-La Roche Ltd, Grenzacherstrasse 124, 4070 Basel, Switzerland
[b] Center for Cellular Imaging and NanoAnalytics (C-CINA), Biozentrum, University of Basel, Mattenstrasse 26, CH-4058 Basel, Switzerland
[c] Roche Diagnostics GmbH, Nonnenwald 2, 82377 Penzberg, Germany
[d] Current address: LeadXpro AG, CH-5234 Villigen, Switzerland

ARTICLE INFO

Article history:
Received 30 September 2015
Received in revised form 10 February 2016
Accepted 11 February 2016
Available online 12 February 2016

Keywords:
Cholesterol transport
Electron microscopy
HDL
LDL
Cholesteryl ester transfer protein
HDL remodeling

ABSTRACT

The cholesteryl ester transfer protein (CETP) enables the transfer of cholesteryl ester (CE) from high-density lipoproteins (HDL) to low-density lipoproteins (LDL) in the plasma compartment. CETP inhibition raises plasma levels of HDL cholesterol; a ternary tunnel complex with CETP bridging HDL and LDL was suggested as a mechanism. Here, we test whether the inhibition of CETP tunnel complex formation is a promising approach to suppress CE transfer from HDL to LDL, for potential treatment of cardio-vascular disease (CVD). Three monoclonal antibodies against different epitopes of CETP are assayed for their potential to interfere with CE transfer between HDL and/or LDL. Surprisingly, antibodies that target the tips of the elongated CETP molecule, interaction sites sterically required to form the suggested transfer complexes, do not interfere with CETP activity, but an antibody binding to the central region does. We show that CETP interacts with HDL, but not with LDL. Our findings demonstrate that a ternary tunnel complex is not the mechanistic prerequisite to transfer CE among lipoproteins.

1. Introduction

Atherosclerotic plaques are a pathological hallmark of cardio-vascular disease (CVD). Their formation is promoted by the accumulation of fatty material, such as cholesterol and triglyceride, in the arterial wall. Cholesterols are poorly water-soluble and are transported in the blood stream by different classes of lipoproteins for delivery to specific tissues: High density lipoproteins (HDLs) contain apolipoprotein A1 (apoA1) as their major protein component, and carry their cholesteryl ester (CE) cargo from peripheral tissues to the liver, where it is either metabolized or re-secreted. Low density lipoproteins (LDLs) and very low density lipoproteins (VLDLs) contain a single copy of apolipoprotein B (apoB), and transport CEs to tissues expressing LDL receptors. CE-rich, oxidized LDLs substantially contribute to plaque formation.

The concentration and distribution of CE in the different lipoprotein classes and among HDL subclasses, depends on the activity of the cholesteryl ester transfer protein (CETP) (Charles and Kane, 2012). In the case of HDL, homotypic transfer of CE by CETP leads to HDL remodeling and the formation of subparticles of various sizes. CETP also mediates heterotypic CE transfer, e.g., from HDL to lipoprotein classes that contain apoB, such as LDL and VLDL (Lagrost et al., 1990; Niesor et al., 2010; Rye et al., 1999). CETP is a potential therapeutic drug target, since its inhibition increases the levels of both HDL-cholesterol and apoA1, which have been shown in numerous epidemiological studies to correlate with decreased CVD risk.

Abbreviations: AUC, analytical ultracentrifugation; apoA1, apolipoprotein A1; apoB, apolipoprotein B; CE, cholesteryl ester; CETP, cholesteryl ester transfer protein; CVD, cardiovascular disease; Fab, fragment antigen binding; GST, glutathione *S*-transferase; HDL, high-density lipoprotein; LDL, low-density lipoprotein; mAb, monoclonal antibody; K_D, dissociation constant; SEC, size exclusion chromatography; SPR, surface plasmon resonance; TEM, transmission electron microscopy; VLDL, very low density lipoprotein.

* Corresponding authors.
E-mail addresses: Eric.Niesor@bluewin.ch (E.J. Niesor), Henning.Stahlberg@unibas.ch (H. Stahlberg).

[1] These authors contributed equally to this work.

http://dx.doi.org/10.1016/j.jsb.2016.02.016
1047-8477/

Whereas the administration of the CETP inhibitor torcetrapib did not benefit CVD patients in a large-scale clinical trial, and was associated with major side effects (Barter et al., 2007), the CETP modulator dalcetrapib (Niesor et al., 2010) was recently found to decrease the risk of CVD in a subgroup of patients with identified single nucleotide polymorphism in the ADCY9 gene (Tardif et al., 2015). In addition, dalcetrapib, but not anacetrapib, was found to increase apoA1-mediated antioxidant uptake in several degenerative diseases, which is potentially protective (Niesor et al., 2014). Two compounds chemically and mechanistically related to torcetrapib, but without its side effects, are currently under investigation in patients suffering from CVDs.

X-ray crystallography showed the 74 kDa protein CETP to be a banana-shaped molecule with a pseudo twofold symmetry: a centrally located N-terminus leads to a β-sheet rich barrel at one tip (here designated N-terminal tip), which is connected via a central domain to a similar, β-sheet rich barrel at the other tip (here designated C-terminal tip), and the fold concludes with a centrally located α-helix at the C-terminus (Qiu et al., 2007). The size and curvature of CETP match those of a discoid HDL particle. Consequently, the concave CETP face was proposed to interact with HDL (Qiu et al., 2007). However, the Ren group recently claimed that CETP may interact with HDL via one of its distal ends (Zhang et al., 2012). Three decades ago, Barter et al. suggested a shuttle lipid-transfer mechanism in which CETP interacts with HDL and is loaded with CE. The cargo would then be shuttled and released by docking of CETP to LDL or VLDL (Barter et al., 1982). According to this shuttle-model, CE molecules would be transported and released one by one, in exchange for neutral lipids such as triglycerides. The model is supported by kinetic studies (Barter and Jones, 1980; Connolly et al., 1996). An alternative model, also based on kinetics, suggests the formation of intermediary CETP, HDL, and LDL collision complexes, and that this proposed complex might be transient (Ihm et al., 1982). The Ren group used transmission electron microscopy (TEM) to study physical mixtures of CETP, HDL and LDL, and concluded that the N-terminal tip domain of CETP binds to HDL and the C-terminal tip to LDL (Zhang et al., 2012). Their study suggests the formation of a transient and/or stationary ternary tunnel complex between CETP, HDL, and LDL or VLDL, where CETP bridges between the two lipoprotein cores to allow transfer of lipid through its inner hydrophobic tunnel. This model implies that CE transfer requires the interaction of one tip of CETP with lipoproteins for efficient CE transfer and, thus, that any disturbance of the interaction of CETP tips with lipoproteins should interfere with CE transfer.

However, a couple of studies have shown that the carboxyl-terminal α-helix of CETP, which is located in the middle of the concave CETP face (Qiu et al., 2007), is involved in lipid transfer: Small peptides restricted to, and derived from, this C-terminal α-helical domain are amphipathic and capable of remodeling lipid mixtures through secondary structure disorder-to-order transitions (Garcia-Gonzalez et al., 2014). A few earlier studies suggested that the carboxyl-terminal α-helix might impact CETP activity, and a series of monoclonal antibodies binding near this region were shown to be inhibitory (Guyard-Dangremont et al., 1999; Swenson et al., 1989; Wang et al., 1992). Atomistic simulations related with to inhibitory action of anacetrapib, suggested the importance of the concave CETP face and the carboxyl-terminal α-helix for CETP activity (Aijanen et al., 2014). Morton and Izem recently demonstrated that CETP is involved in unidirectional lipid transfer without the exchange of neutral lipids (Morton and Izem, 2014).

We have investigated HDL, LDL, CETP and their mixtures by immuno-TEM and biophysical methods, and find that monoclonal antibodies (mAb) directed against either the N or the C terminal tip of CETP do not interfere with the formation of CETP–HDL complexes, and do not interfere with the efficiency of CE transfer between HDL and LDL particles. We also find that the binding of CETP to HDL results in a variety of different CETP–HDL complexes; CETP can bind to HDL via the N-terminal or the C-terminal tip domain. Our results further indicate that the formation of ternary HDL–CETP–LDL tunnel complexes is not a prerequisite for CE transfer, in contradiction to the findings of Zhang et al. (2012).

2. Materials and methods

2.1. Lipoprotein source and preparation protocol

Human LDL and human HDL preparations in 0.15 M NaCl, 0.01% EDTA, pH 7.2 from normolipidemic blood plasma were purchased from Intracel (MD, USA). Discoidal HDL particles were reconstituted (HDL) by the cholate dialysis method as described previously (Ohnsorg et al., 2011). The HDL and LDL used for the AUC experiments was purified from human plasma by density gradient ultracentrifugation (Intracel product information), which allows strong enrichment, but not a quantitative separation of very low-density lipoprotein (VLDL) (density < 1.019 g/ml), LDL (density = 1.019–1.063 g/ml) and HDL (density = 1.063–1.21 g/ml).

2.2. Preparation of CETP

A cell line, expressing recombinant human wild-type CETP, was kindly provided by Professor Alan Tall (Columbia University) (Weinberg et al., 1994). CETP was purified by hydrophobic interaction chromatography and size exclusion chromatography (SEC) according to Ohnishi et al. (1990) with modifications: After SEC chromatography the buffer of the CETP-solution was changed to 20 mM HEPES/NaOH, 10% (w/v) glycerol, 0.02% sodium azide, pH 7.5. CETP was snap-frozen in this buffer and stored at −80 °C.

2.3. Generation of anti-CETP monoclonal Fab fragments

Monoclonal antibodies (mAb), mAb_6/2 and mAb_6/17, were raised as described in Niesor et al. (2010). mAB_JHC1 was obtained from Japan Tobacco as described by Takahashi et al. (2001). Fab fragments were prepared from IgG using a Fab preparation kit from Pierce (product code: 44980). The purity of all preparations was confirmed by high-pressure liquid chromatography (HPLC) and sodium dodecyl sulfate polyacrylamide gel electrophoresis (SDS–PAGE). Fabs were in 20 mM HEPES/NaOH, 50 mM NaCl, pH 7.5. They were snap-frozen and stored at −80 °C.

2.4. Analytical ultracentrifugation (AUC)

Sedimentation velocity data were recorded at 20 °C using a Beckman Coulter XLI analytical ultracentrifuge equipped with an Aviv fluorescence detection system (Kingsbury and Laue, 2011). CETP was labeled with Alexa Fluor 488 at a labeling degree of ~0.8 mol/mol using the Alexa Fluor 488 antibody labeling kit (A20181, Molecular Probes, Life Technologies), with the exception that Zeba spin desalting columns (89882, 7 kDa MWCO, 0.5 ml, Thermo Scientific) were used to removing excess free dye after labeling. To investigate complex formation, 100 nM of Alexa Fluor 488-labeled CETP was incubated with 0.5 mg/ml (protein content) of each human HDL and/or LDL preparation, and centrifuged at 42,000 rpm (An60-Ti rotor; 1.2 cm SedVel60 K centerpieces from Spin Analytical) with fluorescence detection. Absorbance controls for lipoprotein peak allocation were performed at 0.25 mg/ml (protein content) HDL or LDL. Dulbecco's Phosphate Buffered Saline (PBS) (Gibco) was used as buffer in all AUC experiments. Data were analyzed with the programs Sedfit (Schuck, 2000) and Origin (OriginLab), and plotted

with GUSSI (Brautigam, 2015) (http://biophysics.swmed.edu/MBR/software.html) and GraphPad Prism (GraphPad Software).

Due to the complexity of the samples containing HDL or LDL, signal-weighted sedimentation coefficients, sw, of free CETP-Alexa Fluor 488 were compared in the region of 3–4 S. The HDL and LDL concentrations employed were adjusted according to the protein content – LDL particles contain relatively more lipid and also more sites for unspecific interaction with residual free Alexa Fluor 488.

2.5. TEM sample preparation

2.5.1. Investigation of CETP–lipoprotein complex formation

Stock solutions of CETP (0.1 mg/ml) were mixed with pre-diluted HDL (protein-content of the stock solution, 6.8 mg/ml) or pre-diluted LDL (protein-content of the stock solution, 5 mg/ml) at a weight to weight ratio of 5:1, respectively 2:3, and incubated at 37 °C (shaking) for 30 min. CETP/HDL mixtures containing CETP–HDL complexes were mixed with LDL so that the final CETP/HDL/LDL concentrations were 10 μg/ml/2 μg/ml (protein-content)/15 μg/ml (protein-content), and similarly incubated. No additional dilution was required for the TEM experiments.

2.5.2. Fab–CETP and Fab–Fab–CETP complex formation

Solutions of Fab (0.2 mg/ml) and CETP (0.1 mg/ml) were mixed for 1 h at RT at a molar ratio of 2:1 to obtain Fab–CETP complexes, and at a molar ratio of 1:1:0.5 to obtain Fab–Fab–CETP complexes. The mixtures were diluted with PBS to a final protein concentration of 10 μg/ml immediately before TEM analysis.

2.5.3. Fab–CETP–HDL complex formation

Diluted mixtures (final concentration, 5 μg/ml Fab, 2.5 μg/ml CETP) containing Fab–CETP complexes were mixed with diluted solutions of HDL (protein content, 2.0 μg/ml) and incubated for 30 min at RT. No additional dilution was required for the TEM experiments.

All pre-dilutions and dilutions for incubations and TEM analyses were made with PBS, pH = 7.4 (Sigma).

2.6. Analysis by negative stain TEM

5 μL of sample solution was adsorbed for 1 min to glow discharged, parlodion and carbon-film coated TEM grids. Excess sample was removed with blotting paper. The grid was washed 5 times on milliQ water drops, negatively stained with 2% uranyl acetate, blotted again, and air-dried. Images were recorded with a Philips CM10 TEM (FEI Company, Eindhoven, The Netherlands) operated at 80 kV, at a nominal magnification of 130′000×, using a 2 K × 2 K Veleta side-mounted TEM CCD Camera (Olympus), corresponding to a pixel size of 3.8 Å at the specimen level.

2.7. Image processing

Images of 600 particles for HDL, 100 particles for LDL, 200 particles for the Fab–CETP complexes, and 200 particles for the Fab–CETP–HDL complexes were selected manually using the BOXER software (EMAN software package (Ludtke et al., 1999)), and windowed. Particles were classified with the EMAN1 program *startnrclasses*, requesting approximately 50 to 80 particles per class average. Alignment and classification in EMAN1 generated several classes per dataset.

Particle sizes were determined using the ImageJ software (Rasband, 2015).

All visualization and 3D modeling was done using the UCSF Chimera package (Pettersen et al., 2004). The models were prepared by manually selecting the orientations of the three-dimensional (3D) atomic structures that correspond to two-dimensional (2D) projections obtained by single particle analysis (projection matching). Briefly, atomic structures of CETP (PDB code 2ODB) and an individual Fab (obtained from PDB code 1IGY) were displayed in Chimera as all atoms representations on a pale gray background. Views obtained by rotation/translation then look similar to 2D projections and can, thus, be compared and aligned manually with the TEM single particle class averages. Once the optimal orientation of CETP and superimposed Fab was found, the respective atomic coordinates were written out as PDB files. These PDB files were used to produce electron density map surfaces at 20 Å resolution in EMAN (Ludtke et al., 1999), using the command "*pdb2mrc apix* = 1 *res* = 20 *center*". A general constraint was that the final model had to fit all data sets documenting Fab binding to CETP (Figs. 1 and 2 and Supplementary Figs. S2, S3, S5).

2.8. Heterotypic HDL-to-LDL transfer assay using 3H-labeled CE HDL

The inhibitory potency of mAb_6/2, mAb_6/17 and mAb_JHC1 to decrease CE transfer from HDL to LDL by CETP (Roy et al., 1996), was measured using a scintillation proximity assay kit, (#TRKQ7015; GE Healthcare, Waukesha, WI, USA). CE-labeled HDL donor particles were incubated in the presence of purified CETP protein (final concentration, 0.5 μg/ml) and biotinylated LDL acceptor particles for 3 h at 37 °C as described in Barter et al. (Barter and Jones, 1980). Subsequently, streptavidin-coupled polyvinyltoluene beads containing a liquid scintillation cocktail binding selectively to biotinylated LDL were added. The amount of CE transferred to LDL was measured by β counting.

2.9. Heterotypic transfer assay using fluorescently-labeled cholesteryl ester liposomes

The fluorescence-based CETP activity assay kit was obtained from ROAR Biomedical Inc. (New York, USA). The donor liposomes contain CE labeled with the fluorophore NBD [N-(7-nitrobenz-2-oxa-1.3-diazol-4-yl)] in a self-quenched condition (Swenson et al.). These donor liposomes were then incubated with the liposomal acceptor particles in the presence of CETP. CETP-mediated transfer was recognized and determined by measuring the increase in the fluorescence signal intensity. The intensity increases because, in the acceptor particle, the fluorescent lipid is released from the self-quenched donor state. The number of transferred CE molecules is thereby directly proportional to the increase in the fluorescence signal. To measure the inhibitory potency of mAb_6/2, mAb_6/17, mAb_JHC1, each mAb (final concentration, 100 μg/ml) was incubated with CETP (final concentration, 30 μg/ml) for 10 min at RT. 10 μL of this incubate and 4 μL of the donor and acceptor CE liposomal vesicles, were then added to 186 μL of assay buffer. After incubating for 3 h at 37 °C, the increase in fluorescence intensity was measured at an excitation wavelength of 465 nm and an emission wavelength of 535 nm (Tecan Microplate Reader Infinite M200 Pro, Tecan, Maennedorf, Germany). A mouse mAb raised against an irrelevant protein, glutathione *S*-transferases (GST), was used as negative control (mAb control).

2.10. HDL remodeling assay

HDL was incubated with CETP (30 μg/ml) in the presence of 100 μg/ml mAb for 21 h at 37 °C. After the incubation step, the concentration of pre-β-HDL was determined by ELISA (Sekisui Medical Co. Ltd, Tokyo, Japan). The CETP-dependent neutral lipid transfer generated a subclass of HDL, the CE-poor particle known as pre-β-HDL. The amount of pre-β-HDL was then quantified by detecting the exposure of a specific epitope on the apoA1 present, as described by Miida et al. (2003). A mouse mAb raised against an

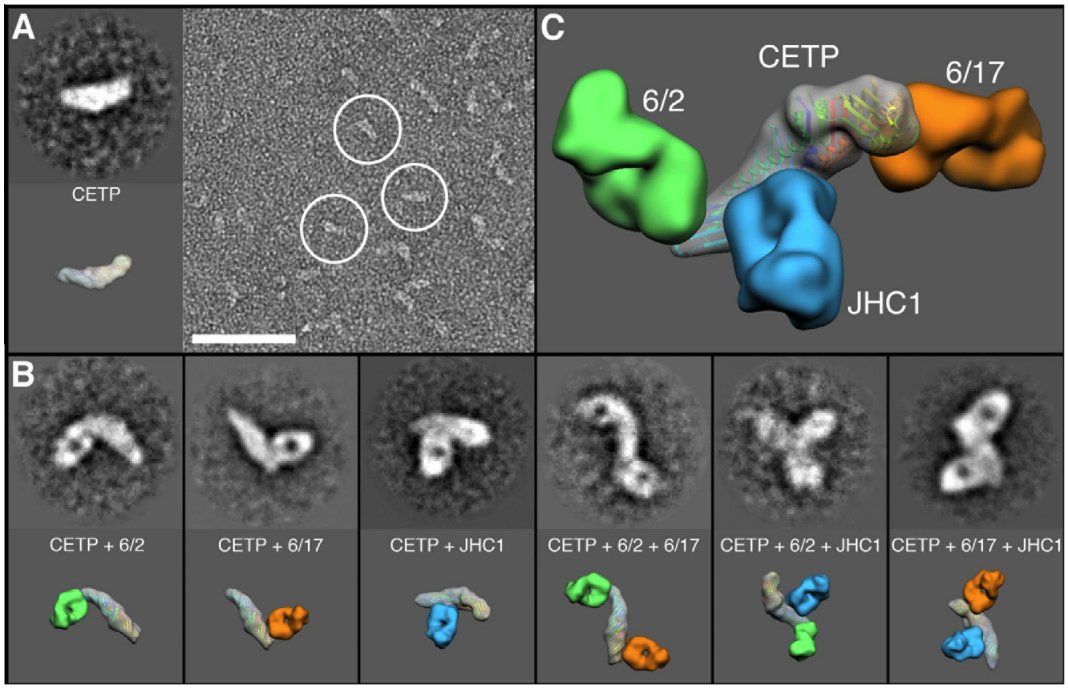

Fig. 1. CETP and immunolabeled CETP imaged by negative stain TEM. (A) CETP. Right: Overview image; the white circles indicate individual CETP molecules. Left: A representative single particle class average (top) and the correspondingly aligned and oriented 20 Å-resolution CETP model generated from the known crystal structure (PDB code: 2OBD) (bottom). See also Supplementary Fig. S1. (B) Class averages (top) and corresponding models displayed as colored density map surfaces (bottom) showing single and double immunolabeling of CETP by the indicated Fabs. See also Supplementary Figs. S2, S3. The proposed models were produced by manual projection matching as described in Section 2. (C) The most probable binding sites for the three Fabs (compare Supplementary Fig. S2 and S3; see Section 2). A rainbow colored ribbon model of CETP (PDB code: 2OBD) is displayed inside a gray transparent density map calculated at 20 Å resolution; the view shows the concave CETP face. Fab fragments (PDB codes 1IGY) are represented as colored opaque density map surfaces at 20 Å resolution. The C-terminal α-helix of CETP is located approximately at the binding site of Fab_JHC1. The often specific and defined angle made by the Fab to the longitudinal CETP axis when adsorbed to the carbon film, served as a guideline for model construction. The double labeling experiments confirmed these angles and showed the relative orientations of the two Fabs. The end assignments are tentative as the epitopes to which the Fabs bind are not known from other methods and the resolution of negative stain TEM does not allow the two ends of the CETP molecule to be distinguished with certainty. This model and all partial models are shown purely as illustrations to aid understanding; the ends to which the Fabs bind are, thus, intentionally not specified. Scale bar: (A) 50 nm; all inset boxes are 30 nm by 30 nm.

irrelevant protein, GST, was used as negative control (mAb control).

2.11. Binding characterization by SPR spectroscopy

SPR experiments were performed using a capture assay method to determine mAb–protein interactions and binding affinities (Biacore Instruments). Goat anti-mouse mAbs were covalently immobilized on the sensor chip surface by amine coupling. The antibodies mAb_6/2, mAb_6/17 and mAb_JHC1, were then captured for the binding assay (ca. 150–300 RU of captured antibody). Subsequently, different CETP concentrations were injected and passed over the chip surface at a flow rate of 50 µL/min. Surface regeneration with 100 mM phosphoric acid was performed after each injection. The experiments were carried out at 25 °C using a 5 mM Hepes pH 7.5, 50 mM NaCl, 5% glycerol, 0.01% P20 running buffer.

3. Results

Analysis of recombinant human CETP by negative stain TEM confirmed the banana-like shape of the protein (Figs. 1A and S1) (Qiu et al., 2007). At the 20 Å resolution achievable by this method, the two halves of the 13-nm-long, curved structure look similar. Immunolabeling was used to locate specific CETP domains. The required precision was attained by using the fragment antigen-binding regions (Fabs; Supplementary Fig. S2) of monoclonal antibodies (mAbs) against CETP; Fabs bind to target proteins by the same, well-defined interaction as the full mAbs, but the stiff structures of the smaller Fabs allow image processing, while the more flexible full-length antibodies do not (Wu et al., 2012). Importantly, as in full-length antibodies, the characteristic projections of Fabs that lie flat or almost flat on the support film (Supplementary Fig. S1B) allow them to be unambiguously identified by negative stain TEM. It is known from studies using ELISA, that each of the three mAbs employed, mAb_6/2, mAb_6/17 and mAb_JHC1, binds to and masks a different epitope on the CETP surface (Niesor et al., 2010). Surface plasmon resonance (SPR) spectroscopy used to determine the dissociation constants (K_D) of mAb/CETP complexes showed that mAb_JHC1 has the lowest affinity of the three: K_D of mAb_6/2 = 0.001 nM, K_D of mAb_6/17 = 0.7 nM and K_D of mAb_JHC1 = 40 nM. TEM images of negatively stained CETP labeled by Fab_6/2 (from mAb_6/2) and Fab_6/17 (from mAb_6/17) alone (Figs. 1B,C and S2A,B) and in combination (Supplementary Fig. S3A), confirm that the two Fabs bind at different epitopes (Niesor et al., 2010) and show these to be at opposite tips of the CETP molecule. Similar TEM experiments showed that Fab_JHC1 (from mAb_JHC1) binds to the concave surface (Figs. 1B,C and S2C), closer to the binding site of Fab_6/2 than to the binding site of Fab_6/17 (Figs. 1B,C and S3B,C).

As shown by both analytical ultracentrifugation (AUC; Fig. 2) and TEM (Fig. 3), CETP-HDL complexes formed when CETP was mixed with HDL as indicated in Section 2. In the TEM images, the circular projections typical of HDL (Supplementary Fig. S4A) are frequently extended by an elongated protrusion with the shape of CETP but usually one third shorter (Figs. 3A and S4B). The overall shapes of CETP, HDL, and the CETP–HDL complexes agree with those reported by Zhang et al. (2012). Multiple CETP binding

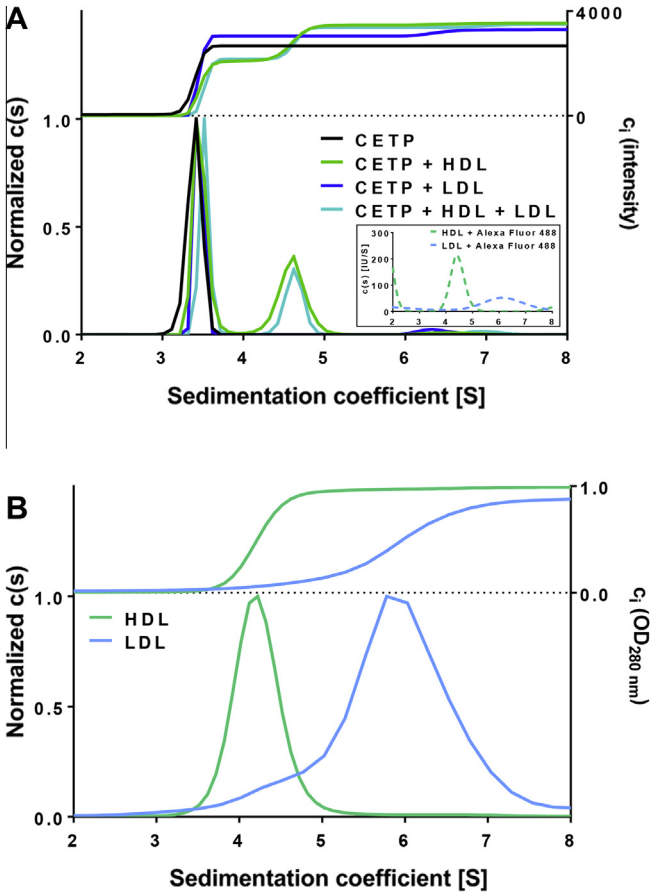

Fig. 2. Normalized sedimentation coefficient distributions c(s) determined by analytical ultracentrifugation (AUC). (A) The sedimentation of 100 nM CETP labeled with Alexa Fluor 488 followed by fluorescence detection, carried out in the absence and presence of HDL, LDL or an HDL/LDL mixture (0.5 mg/ml protein each). CETP readily formed a complex with HDL (peak at 4.6 S) but not with LDL; the total fluorescence signal/quantum yield of CETP-Alexa Fluor 488 was markedly increased in the presence of LDL compared to HDL. The sedimentation of the HDL–CETP complex is dominated by the HDL particle, addition of more than one CETP to HDL is not expected to markedly change the sedimentation coefficient, consequently the stoichiometry of the HDL–CETP complex(es) cannot be inferred from the data. The signal-weighted sedimentation coefficients, sw, of free CETP-Alexa Fluor 488 in the 3–4 S region are the same for all samples. Inset: AUC control experiment. This was performed with 10 nM Alexa Fluor 488 in presence of either HDL or LDL (0.5 mg/ml protein each). The profiles show that residual free Alexa Fluor 488 stains both HDL and LDL, which explains the occurrence of the minor peaks at 6–7 S in the main graph. (B) AUC control experiment. Sedimentation of 0.25 mg/ml HDL or LDL in the absence of CETP detected by the absorbance at 280 nm. The upper panels of (A) and (B) show the integrated distributions (total loading signals.)

stoichiometries were also evident, with up to five CETP molecules binding to the same HDL particle ((Zhang et al., 2012), and Figs 3A and S4B). Neither ternary HDL–CETP–HDL complexes nor higher stoichiometries were observed (Supplementary Fig. S4B). Occasionally, a second HDL was observed in close proximity to an HDL–CEPT complex, and very rarely HDL–CETP clusters were seen, as always expected due to adsorption artifacts. Pure HDL–CETP complexes were repeatedly observed on negatively stained TEM grids (considered further below).

To further investigate how CETP interacts with HDL, HDL was incubated with solutions containing Fab_6/2–CETP, Fab_6/17–CETP, or Fab_JHC1–CETP complexes, and inspected by negative stain TEM. Many labeled CETP–HDL complexes were visible in samples containing Fab_6/2 or Fab_6/17 and most of these particles had a similar shape, allowing statistical analysis by image processing in both cases (Figs. 3B,C and S5A,B). Surprisingly, the data reveal that CETP is able to bind HDL via either its N- or C-terminal tip. The CETP–HDL complexes were less frequently labeled by Fab_JHC1, prohibiting statistically meaningful image processing. Nevertheless, when labeling was evident, the Fab_JHC1 was directly adjacent to the HDL particle (Figs. 3 and S5C).

To investigate the potential interaction of CETP with LDL (Fig. 4A), mixtures of CETP and LDL were prepared as above and analyzed by AUC and negative stain TEM. According to the AUC data, significant complex formation was observed for CETP in the presence of HDL, but not in the presence of LDL (Fig. 2). A control experiment demonstrated that the free Alexa Fluor 488 dye could interact with HDL and LDL particles (Fig. 2A, inset). The CETP-Alexa Fluor 488 inevitably contained residual free dye. Thus, the very minor peaks at 6–7 S (on average 4.2% of total signal) in the sedimentation coefficient distributions shown in Fig. 2A cannot be attributed to complexes consisting of CETP and LDL, but are rather due to unspecific interaction of residual free dye with LDL. In agreement, only randomly distributed free CETP particles and free LDL particles were found on the TEM grids; CETP–LDL complexes were not detected (Fig. 4B). This observation contradicts the report by the Ren group from 2012 (Zhang et al., 2012). Further, physically stable ternary complexes of HDL–CETP–LDL were not detected by AUC (Fig. 2) when a mixture of CETP and HDL complexes was incubated at room temperature with LDL. On corresponding TEM grids, HDL was occasionally in very close proximity to LDL (Fig. 4C). At first sight, these aggregates could be interpreted as ternary complexes. However, a simulation of the adsorption process occurring when grids are prepared for negative stain TEM from heterogeneous HDL/CETP/LDL samples generated the same forms (Supplementary Fig. S6), clearly indicating that the apparent complexes are most likely adsorption artefacts. This conclusion differs from that of Zhang et al. (2012). The formation of CETP–HDL complexes and the absence of CETP–LDL and HDL–CETP–LDL documented by the above data (Figs. 2 and 4) implies that any interaction that CETP might have with LDL is transient as suggested by Morton and Greene (2003), and does not result in the formation of a stable isolatable complex.

Inhibition of neutral lipid transfer by mAb_6/2, mAb_6/17 and mAb_JHC1, which correspond to Fab_6/2, Fab_6/17 and Fab_JHC1 used for TEM immunolabeling, was studied in three different and independent assays (Table 1). These were a heterotypic HDL-to-LDL transfer assay that determined the transfer of radiolabeled CE from HDL to LDL (Fig. 5A), a heterotypic vesicle-based transfer assay that measured the transfer of a fluorescent CE analog from donor to acceptor phospholipid vesicles (Fig. 5B), and a homotypic HDL-to-HDL transfer assay that measured CETP-dependent HDL remodeling by incubating HDL with CETP and quantifying the generation of pre-β-HDL using a specific ELISA procedure (Fig. 5C). Surprisingly, in all three assays, the monoclonal antibodies mAb_6/2 and mAb_6/17, which bind to the tip-regions of CETP (Figs. 1B,C and S2A,B), had no detectable effect on lipid transfer. In contrast, inhibition of lipid transfer was observed with mAb_JHC1, which binds to an epitope close to the center of the concave CETP face near the α-helical C-terminus (Figs. 1B,C and S2C). The comparatively high K_D of mAb_JHC1 of 40 nM makes the inhibition observed with this mAb even more striking.

4. Discussion

The main results can be summarized as follows: (i) a significant amount of ternary HDL–CETP–LDL complexes was not detected by AUC, (ii) mAbs binding to epitopes in the tip region of CETP that were expected to hinder the formation of the HDL–CETP–LDL ternary tunnel complexes, had poor CETP inhibitory potency, and (iii) according to both the AUC and TEM data, CETP preferentially interacts with HDL. Indeed, TEM indicated that multi-stoichiometric

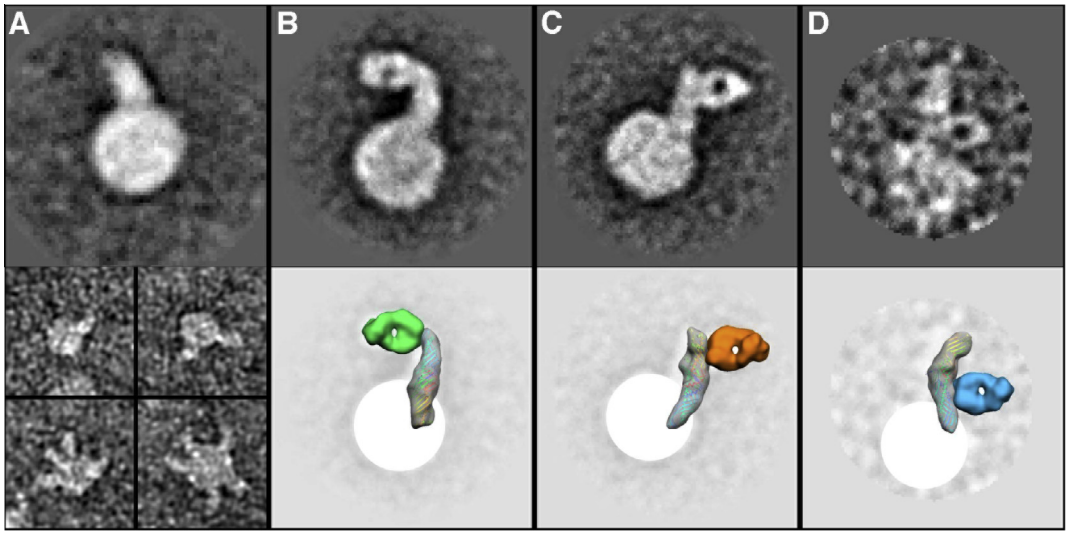

Fig. 3. CETP–HDL complexes and their immunolabeling. Either unlabeled CETP or preformed Fab–CETP complexes were incubated with HDL at 37 °C. The mixture was then imaged by negative stain TEM. (A) CETP–HDL. (B) (Fab_6/2–CETP)–HDL. (C) (Fab_6/17–CETP)–HDL. (D) (Fab_JHC1–CETP)–HDL. Top row: (A–C), representative class averages generated by single particle analysis, (D) single raw image. Bottom row, (A) single raw images showing single and multiple binding of CETP to HDL particles, (B,C) models corresponding to the above averages, rendered as colored density map surfaces at a resolution of 20 Å; the circular HDL projections have diameters of 16–18 nm and about one third of the CETP molecules are attached to them. The large boxes are 38 by 38 nm and the small boxes in (A) 48 by 48 nm.

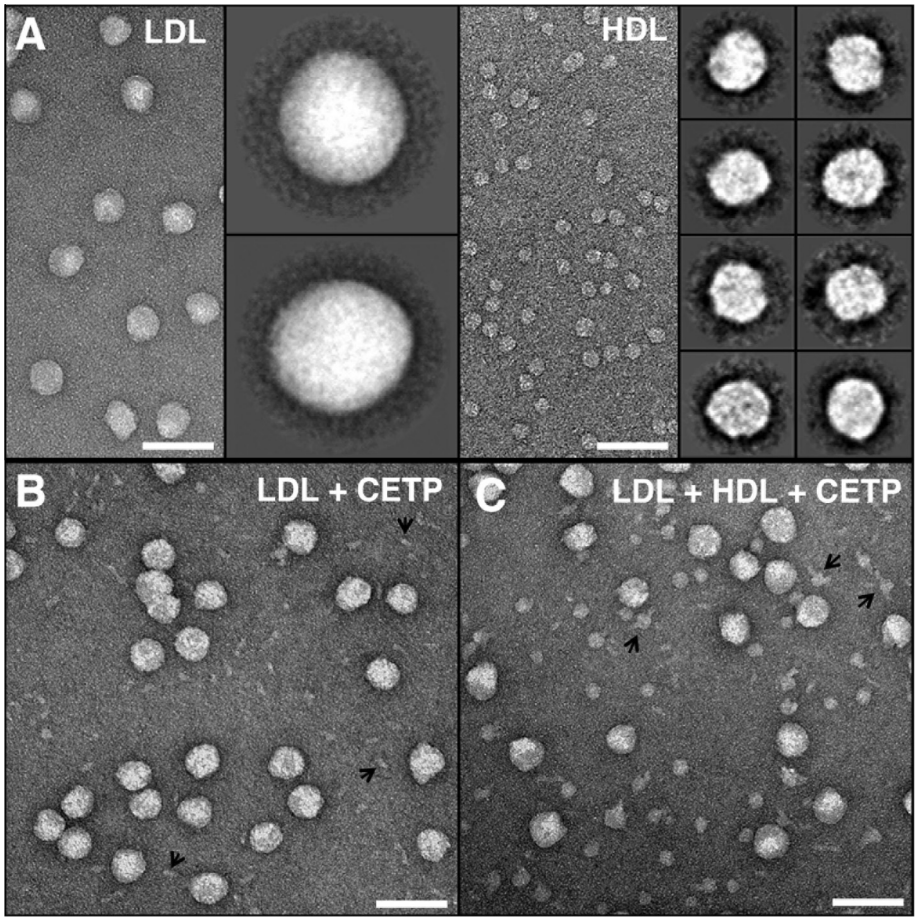

Fig. 4. Interaction of CETP with HDL, LDL and HDL/LDL mixtures studied by TEM. (A) Overview of a 500 times diluted LDL stock solution (5 mg/ml) and 2 representative class averages, each containing ~30 particles (left), and overview of a 5000 times diluted HDL stock solution (7.4 mg/ml) and 8 representative class averages, each containing ~50 particles (right); for comparison with (B) and (C). The average LDL diameter ranged from 38 to 42 nm and the average HDL diameter from 16 to 18 nm. Thus, LDL and HDL can easily be distinguished in mixed samples. (B) CETP and LDL; CETP–LDL complexes were not detected. Unbound individual CETP molecules are visible in the background (arrows). (C) CETP–HDL and LDL. The CETP–HDL complexes are clearly visible (arrows) and some HDL and LDL particles are close to one another or even in contact, giving the impression that they might be ternary CETP–HDL–LDL complexes. However, a simulation shows that this apparent association is most probably an adsorption artifact; see Supplementary Fig. S6. Scale bars: 60 nm; inset boxes are 48 by 48 nm (left) and 24 by 24 nm (right).

Table 1
Summary of the neutral lipid transfer inhibitory potency of mAbs_6/2, mAb_6/17 and mAb_JHC1, which correspond to the Fabs used in the TEM immunolabeling experiments.

	Binding site on CETP	Heterotypic transfer (^{3}H-CE-labeled HDL assay)	Heterotypic transfer (NBD-CE-labeled liposomes assay)	Homotypic transfer (HDL remodeling assay)
mAb_6/2	Tip region	No effect	No effect	No effect
mAb_6/17	Opposite tip region	No effect	No effect	No effect
mAb_JHC-1	Middle of concave side	Inhibition	Inhibition	Inhibition

assemblies of CETP with HDL are possible, but did not reveal CETP–LDL complexes. Moreover, there was no evidence that CETP binds to HDL exclusively by either its N- or its C-terminal tip. Antibody fragments Fab_6/2 and Fab_6/17 label opposite ends of the structure, as shown by double immunolabeling of CETP, and, in agreement with the corresponding mAb experiments, neither Fab prevented the interaction of CETP with HDL particles. The formation of CETP–HDL complexes and the lack of significant amounts of CETP–LDL (Figs. 2 and 4B) and HDL–CETP–LDL complexes (Fig. 2), is supported by size exclusion chromatography; CETP elutes in the HDL peak and in the apolipoprotein-free peak, but is not present in the LDL or the VLDL peak (Dernick et al., 2011). From this and the new TEM results reported above, we conclude that an interaction of CETP with LDL can only be transient at best (Morton and Greene, 2003). These TEM results were unexpected. Together, they indicate that the inhibition of a ternary HDL–CETP–LDL tunnel complex may not be an efficient strategy to suppress CETP-mediated heterotypic lipid transfer.

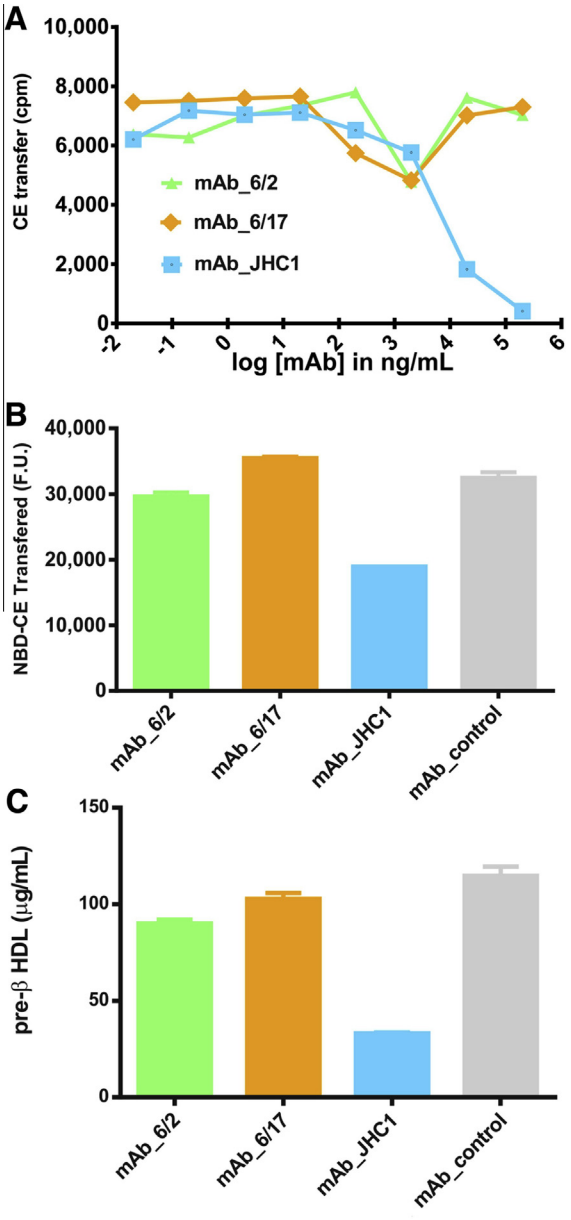

Fig. 5. Neutral lipid transfer inhibitory potency of mAbs_6/2, mAb_6/17 and mAb_JHC1, which correspond to the Fabs used for TEM labeling. (A) Heterotypic transfer of radiolabeled CE from HDL to LDL. (B) Heterotypic transfer of fluorescent CE from donor to acceptor liposomal vesicles. (C) Remodeling of HDL and the formation of pre-β HDL during homotypic transfer. Only the monoclonal antibody mAB_JHC1 shows significant inhibitory potency.

Homotypic transfer (HDL remodeling) due to interaction of CETP with HDL is likely to be a necessary step, even for heterotypic lipid exchange. This is suggested by two findings. (i) Complexes of CETP–HDL are observed in the absence and presence of LDL. (ii) The inhibitory potencies of mAb_6/2, mAb_6/17 and mAb_JHC1 on HDL remodeling, and in the complete absence of LDL, directly correlate to their effect on heterotypic transfer; in both cases mAb_JHC1 inhibits transfer, but mAb_6/2 and mAb_6/17 do not. LDL particles could therefore be seen as lipid reservoirs competing with the distribution of lipids among different HDL subclasses. In this model, the presence of LDL would scavenge CE and other lipids from HDL and promote the release of apoA1 (Liang et al., 1994).

The unexpected ability of CETP to bind to HDL via either its N- or C-terminal tip introduces dissimilarity into otherwise comparably structured CETP–HDL particles. Such differently structured complexes might have slightly different binding properties. Intriguingly, ternary HDL–CETP–HDL complexes were not detected, even though multiple copies of CETP can interact with a single HDL particle (Figs. 3A and S4B). The size, stability, and structure of HDL is known to depend to a large extent on its cholesterol content, implying that any transfer of CE and lipids stabilizes or destabilizes different forms of HDL and/or CETP–HDL complexes (Auton et al., 2013). As short-lived transient complexes in such heterogeneous, dynamic and complex mixtures are difficult to detect by any analytical method, the possible transient and mechanistic scenarios remain a matter of speculation. However, it is a broadly accepted concept that the physical stability of lipid particles and membranes is generally balanced by the adhesion of proteins or amphipathic peptides, and that a change in the particle surface/volume ratio is a general trigger of lipid remodeling processes (McMahon and Gallop, 2005). In principle, such a mode of action might already be sufficient to explain the transfer of lipids from one lipoprotein complex to another. To a certain degree, this is supported by the fact that small-molecule peptides derived from the C-terminal α-helix of CETP are amphipathic and – like CETP – capable of remodeling lipid mixtures (Garcia-Gonzalez et al., 2014). Further, molecules and antibodies that bind near the C-terminal α-helix of CETP, interfere with CE transfer (Maugeais et al., 2013; Swenson et al., 1989; Wang et al., 1992). In agreement, the inhibiting antibody employed in the presented study, mAb_JHC1, binds near this α-helix on the central concavely-curved region of CETP.

5. Conclusions

The static TEM data, and the lipid transfer efficiencies of CETP in the presence of inhibiting and non-inhibiting mAbs, do not allow

conclusions to be drawn about the transient states mechanistically required to transfer CE between lipoproteins: a shuttle mechanism or even a transient short-lived ternary collision complex, which can involve differently constituted and destabilized forms of HDL, HDL–CETP and LDL, are possible (Barter and Jones, 1980; Barter et al., 1982; Connolly et al., 1996; Ihm et al., 1982). However, our data show that the impact of ternary tunnel complexes (HDL–CETP–LDL), if they are formed at all, must be minor. The functional impact of the N- or C-terminal CETP tip domains protruding from CETP–HDL complexes appears to be secondary in the sense that mAbs targeting them neither interfere with the homotypic nor with the heterotypic transfer activity of CETP. This is corroborated by the fact that we could not document the formation of stable HDL–CETP–LDL and HDL–CETP–HDL complexes. The monoclonal antibodies described here, mAb_6/2, mAb_6/17, and mAb_JHC-1, are powerful tools to further unravel the highly dynamic and complex binding scenario underlying CETP-mediated transfer of CE among lipoproteins.

Acknowledgements

We thank Francis Müller and Eric Kusznir for AUC analyses, and Andrea Wiget and Walter Huber for SPR analyses. This work was in part supported by the Swiss Systems Biology initiative SystemsX.ch (RTD grant CINA).

Appendix A. Supplementary data

Supplementary data associated with this article can be found, in the online version, at http://dx.doi.org/10.1016/j.jsb.2016.02.016.

References

Aijanen, T., Koivuniemi, A., Javanainen, M., Rissanen, S., Rog, T., Vattulainen, I., 2014. How anacetrapib inhibits the activity of the cholesteryl ester transfer protein? Perspective through atomistic simulations. PLoS Comput. Biol. 10, e1003987.

Auton, M., Bassett, G.R., Gillard, B.K., Pownall, H.J., 2013. Free cholesterol determines reassembled high-density lipoprotein phospholipid phase structure and stability. Biochemistry 52, 4324–4330.

Barter, P.J., Jones, M.E., 1980. Kinetic studies of the transfer of esterified cholesterol between human plasma low and high density lipoproteins. J. Lipid Res. 21, 238–249.

Barter, P.J., Hopkins, G.J., Gorjatschko, L., Jones, M.E., 1982. A unified model of esterified cholesterol exchanges between human plasma lipoproteins. Atherosclerosis 44, 27–40.

Barter, P.J., Caulfield, M., Eriksson, M., Grundy, S.M., Kastelein, J.J., Komajda, M., Lopez-Sendon, J., Mosca, L., Tardif, J.C., Waters, D.D., Shear, C.L., Revkin, J.H., Buhr, K.A., Fisher, M.R., Tall, A.R., Brewer, B., Investigators, I., 2007. Effects of torcetrapib in patients at high risk for coronary events. N. Engl. J. Med. 357, 2109–2122.

Brautigam, C.A., 2015. Calculations and publication-quality illustrations for analytical ultracentrifugation data. Methods Enzymol. 562, 109–133.

Charles, M.A., Kane, J.P., 2012. New molecular insights into CETP structure and function: a review. J. Lipid Res. 53, 1451–1458.

Connolly, D.T., McIntyre, J., Heuvelman, D., Remsen, E.E., McKinnie, R.E., Vu, L., Melton, M., Monsell, R., Krul, E.S., Glenn, K., 1996. Physical and kinetic characterization of recombinant human cholesteryl ester transfer protein. Biochem. J. 320 (Pt 1), 39–47.

Dernick, G., Obermüller, S., Mangold, C., Magg, C., Matile, H., Gutmann, O., von der Mark, E., Handschin, C., Maugeais, C., Niesor, E.J., 2011. Multidimensional profiling of plasma lipoproteins by size exclusion chromatography followed by reverse-phase protein arrays. J. Lipid Res. 52, 2323–2331.

Garcia-Gonzalez, V., Gutierrez-Quintanar, N., Mendoza-Espinosa, P., Brocos, P., Pineiro, A., Mas-Oliva, J., 2014. Key structural arrangements at the C-terminus domain of CETP suggest a potential mechanism for lipid-transfer activity. J. Struct. Biol. 186, 19–27.

Guyard-Dangremont, V., Tenekjian, V., Chauhan, V., Walter, S., Roy, P., Rassart, E., Milne, A.R., 1999. Immunochemical evidence that cholesteryl ester transfer protein and bactericidal/permeability-increasing protein share a similar tertiary structure. Protein Sci. 8, 2392–2398.

Ihm, J., Quinn, D.M., Busch, S.J., Chataing, B., Harmony, J.A., 1982. Kinetics of plasma protein-catalyzed exchange of phosphatidylcholine and cholesteryl ester between plasma lipoproteins. J. Lipid Res. 23, 1328–1341.

Kingsbury, J.S., Laue, T.M., 2011. Fluorescence-detected sedimentation in dilute and highly concentrated solutions. Methods Enzymol. 492, 283–304.

Lagrost, L., Gambert, P., Dangremont, V., Athias, A., Lallemant, C., 1990. Role of cholesteryl ester transfer protein (CETP) in the HDL conversion process as evidenced by using anti-CETP monoclonal antibodies. J. Lipid Res. 31, 1569–1575.

Liang, H.Q., Rye, K.A., Barter, P.J., 1994. Dissociation of lipid-free apolipoprotein A-I from high density lipoproteins. J. Lipid Res. 35, 1187–1199.

Ludtke, S.J., Baldwin, P.R., Chiu, W., 1999. EMAN: semiautomated software for high-resolution single-particle reconstructions. J. Struct. Biol. 128, 82–97.

Maugeais, C., Perez, A., von der Mark, E., Magg, C., Pflieger, P., Niesor, E.J., 2013. Evidence for a role of CETP in HDL remodeling and cholesterol efflux: role of cysteine 13 of CETP. Biochim. Biophys. Acta 1831, 1644–1650.

McMahon, H.T., Gallop, J.L., 2005. Membrane curvature and mechanisms of dynamic cell membrane remodelling. Nature 438, 590–596.

Miida, T., Miyazaki, O., Nakamura, Y., Hirayama, S., Hanyu, O., Fukamachi, I., Okada, M., 2003. Analytical performance of a sandwich enzyme immunoassay for pre beta 1-HDL in stabilized plasma. J. Lipid Res. 44, 645–650.

Morton, R.E., Greene, D.J., 2003. CETP and lipid transfer inhibitor protein are uniquely affected by the negative charge density of the lipid and protein domains of LDL. J. Lipid Res. 44, 2287–2296.

Morton, R.E., Izem, L., 2014. Cholesteryl ester transfer proteins from different species do not have equivalent activities. J. Lipid Res. 55, 258–265.

Niesor, E.J., Magg, C., Ogawa, N., Okamoto, H., von der Mark, E., Matile, H., Schmid, G., Clerc, R.G., Chaput, E., Blum-Kaelin, D., Huber, W., Thoma, R., Pflieger, P., Kakutani, M., Takahashi, D., Dernick, G., Maugeais, C., 2010. Modulating cholesteryl ester transfer protein activity maintains efficient pre-beta-HDL formation and increases reverse cholesterol transport. J. Lipid Res. 51, 3443–3454.

Niesor, E.J., Kallend, D., Bentley, D., Kastelein, J.J., Kees Hovingh, G., Stroes, E.S., 2014. Treatment of low HDL-C subjects with the CETP modulator dalcetrapib increases plasma campesterol only in those without ABCA1 and/or ApoA1 mutations. Lipids 49, 1245–1249.

Ohnishi, T., Yokoyama, S., Yamamoto, A., 1990. Rapid purification of human plasma lipid transfer proteins. J. Lipid Res. 31, 397–406.

Ohnsorg, P.M., Mary, J.L., Rohrer, L., Pech, M., Fingerle, J., von Eckardstein, A., 2011. Trimerized apolipoprotein A-I (TripA) forms lipoproteins, activates lecithin:cholesterol acyltransferase, elicits lipid efflux, and is transported through aortic endothelial cells. Biochem. Biophys. Acta – Mol. Cell Biol. Lipids 1811, 1115–1123.

Pettersen, E.F., Goddard, T.D., Huang, C.C., Couch, G.S., Greenblatt, D.M., Meng, E.C., Ferrin, T.E., 2004. UCSF Chimera–a visualization system for exploratory research and analysis. J. Comput. Chem. 25, 1605–1612.

Qiu, X., Mistry, A., Ammirati, M.J., Chrunyk, B.A., Clark, R.W., Cong, Y., Culp, J.S., Danley, D.E., Freeman, T.B., Geoghegan, K.F., Griffor, M.C., Hawrylik, S.J., Hayward, C.M., Hensley, P., Hoth, L.R., Karam, G.A., Lira, M.E., Lloyd, D.B., McGrath, K.M., Stutzman-Engwall, K.J., Subashi, A.K., Subashi, T.A., Thompson, J. F., Wang, I.K., Zhao, H., Seddon, A.P., 2007. Crystal structure of cholesteryl ester transfer protein reveals a long tunnel and four bound lipid molecules. Nat. Struct. Mol. Biol. 14, 106–113.

Rasband, W.S., 2015. ImageJ. U.S. National Institutes of Health, Bethesda, Maryland, USA, http://imagej.nih.gov/ij/, 1997–2015.

Roy, P., MacKenzie, R., Hirama, T., Jiang, X.C., Kussie, P., Tall, A., Rassart, E., Milne, R., 1996. Structure-function relationships of human cholesteryl ester transfer protein: analysis using monoclonal antibodies. J. Lipid Res. 37, 22–34.

Rye, K.A., Clay, M.A., Barter, P.J., 1999. Remodelling of high density lipoproteins by plasma factors. Atherosclerosis 145, 227–238.

Schuck, P., 2000. Size-distribution analysis of macromolecules by sedimentation velocity ultracentrifugation and Lamm equation modeling. Biophys. J. 78, 1606–1619.

Swenson, T.L., Hesler, C.B., Brown, M.L., Quinet, E., Trotta, P.P., Haslanger, M.F., Gaeta, F.C., Marcel, Y.L., Milne, R.W., Tall, A.R., 1989. Mechanism of cholesteryl ester transfer protein inhibition by a neutralizing monoclonal antibody and mapping of the monoclonal antibody epitope. J. Biol. Chem. 264, 14318–14326.

Takahashi, H., Takahashi, A., Maki, M., Sasai, H., Kamada, M., 2001. Effect of CETP on the plasma lipoprotein profile in four strains of transgenic mouse. Biochem. Biophys. Res. Commun. 283, 118–123.

Tardif, J.C., Rheaume, E., Lemieux Perreault, L.P., Gregoire, J.C., Feroz Zada, Y., Asselin, G., Provost, S., Barhdadi, A., Rhainds, D., L'Allier, P.L., Ibrahim, R., Upmanyu, R., Niesor, E.J., Benghozi, R., Suchankova, G., Laghrissi-Thode, F., Guertin, M.C., Olsson, A.G., Mongrain, I., Schwartz, G.G., Dube, M.P., 2015. Pharmacogenomic determinants of the cardiovascular effects of dalcetrapib. Circ. Cardiovasc. Genet. 8, 372–382.

Wang, S., Deng, L., Milne, R.W., Tall, A.R., 1992. Identification of a sequence within the C-terminal 26 amino acids of cholesteryl ester transfer protein responsible for binding a neutralizing monoclonal antibody and necessary for neutral lipid transfer activity. J. Biol. Chem. 267, 17487–17490.

Weinberg, R.B., Cook, V.R., Jones, J.B., Kussie, P., Tall, A.R., 1994. Interfacial properties of recombinant human cholesterol ester transfer protein. J. Biol. Chem. 269, 29588–29591.

Wu, S., Avila-Sakar, A., Kim, J., Booth, D.S., Greenberg, C.H., Rossi, A., Liao, M., Li, X., Alian, A., Griner, S.L., Juge, N., Yu, Y., Mergel, C.M., Chaparro-Riggers, J., Strop, P., Tampe, R., Edwards, R.H., Stroud, R.M., Craik, C.S., Cheng, Y., 2012. Fabs enable single particle cryoEM studies of small proteins. Structure 20, 582–592.

Zhang, L., Yan, F., Zhang, S., Lei, D., Charles, M.A., Cavigiolio, G., Oda, M., Krauss, R.M., Weisgraber, K.H., Rye, K.A., Pownall, H.J., Qiu, X., Ren, G., 2012. Structural basis of transfer between lipoproteins by cholesteryl ester transfer protein. Nat. Chem. Biol. 8, 342–349.